Contents lists available at ScienceDirect

Toxicology Reports

Full length article

UVB damage onset and progression 24 h post exposure in human-derived skin cells

Christian Khalil[a,b,*], Wassim Shebaby[a]

[a] School of Arts and Sciences, Department of Natural Sciences, Lebanese American University (LAU), Byblos, Lebanon
[b] Institute of Environmental Studies, University of New South Wales (UNSW), Sydney, Australia

ARTICLE INFO

ABSTRACT

The focus of this research was on UVB radiation (280–320 nm) responsible for cellular changes in skin of acute and chronically exposed individuals. This study investigated the acute cellular damages triggered by UVB exposure of cultured human fibroblasts and keratinocyte cells immediately and 24 h post exposure in order to understand damage onset and progression. The study evaluated a number of cellular parameters including mitochondria, lysosomes, cell membrane, DNA damages as well as pro and anti-apoptotic protein expression levels. Cellular organelle damages were assessed by a battery of in vitro toxicological assays using MTS and Neutral red cytotoxicity assays. Cell membrane damages were also assessed by measuring lactate dehydrogenase (LDH) enzyme leakage from UVB exposed cells. Lastly DNA damages was assessed using the comet assay while protein expression was evaluated using Western Blot.

In this study we reported in all our assay systems (MTS, NR and LDH) that cellular damages were UVB dose dependent with damages amplified 24 h post exposure. Our results also indicated that incubation of exposed cells for a period of 24 h increased the sensitivity of the assay systems used. The increased sensitivity in detecting early cytotoxic damages was manifested though organelle damage measurement at very low doses which were not manifested immediately post exposure. The data also indicated that HaCaT cells were most sensitive in detecting UVB triggered damages immediately and 24 h post exposure using the MTS assay. We also established upregulation and downregulation of various apoptotic proteins at various time points post exposure. The presented data clearly indicated the need for a comprehensive assessment of UVB damages 4 and 24 h post exposure due to the different assay sensitivities in addition to various signaling mechanisms activated at different time points post exposure.

1. Introduction

Ultraviolet radiation represents one of the important contributing factors to cellular damages and cancer onset in human exposed skin. UV exposure especially in the UVB (280–320 nm) range is the main cause for malignant cancer developments and is responsible for many deaths worldwide [1]. UVB radiation can penetrate the upper layers of the skin and reach the dermis [2,3]. This ability to penetrate skin layers contributes to damaging major skin cell populations from keratinocytes to fibroblasts. Strong evidence suggests that UVB induces damage, resulting in skin cell loss and/or apoptosis [4,5]. It is assumed that keratinocytes are the most numerous cells in human skin and likely the first cells to be damaged by UV radiation [6]. Previous studies in the literature also indicated that exposure of skin cells to UVB radiation induced various cell modifications including formation of reactive oxygen species (ROS) [3,7], cell cycle arrest and activation of numerous

cell genes and cell markers [8]. ROS generation induces membrane disruption as well as nuclear DNA damage leading to apoptotic cell death [9]. Mounting evidence also suggested that UVB-induced apoptosis in keratinocytes is mediated through several independent signaling pathways [3] mainly death receptor activation (extrinsic pathway) [10,11], mitochondrial intrinsic pathway [12] and mitogen-activated protein kinases (MAPKs) [13].

We have previously reported in [14] a good correlation between the MTS and NR assays in measuring UVB damages in exposed cells immediately post exposure. This correlation could not be observed 24 h post exposure hence the need for further investigations to elucidate the underlying mechanisms of UVB induced cellular damages. The present study represents a novel approach in assessing cellular organelles specific damages triggered by UVB exposure. The aim of this study is to elucidate cellular damages onset immediately post exposure and its progression 24 h post exposure. This was achieved by using a range of

---

* Corresponding author at: School of Arts and Sciences, Department of Natural Sciences, Lebanese American University (LAU), Byblos, Lebanon.
E-mail addresses: Christian.khalil@lau.edu.lb, c.khalil@unsw.edu.au (C. Khalil).

cytotoxicity techniques investigating a number of cell endpoints, ranging from membrane damages, mitochondrial dehydrogenase activity, lysosomal disruption, DNA damages.

2. Material and methods

2.1. Cell cultures and their maintenance

Cell cultures (passage number 30–35) were maintained in DMEM (Dulbecco's modified essential medium; Gibco, USA) medium supplemented with 5% (v/v) fetal calf serum (JS Bioscience, Australia), L-glutamine (2 mM), penicillin (100 Uml-1) and streptomycin (0.1 mg ml-1; Sigma, USA). Culture cells were kept at 37 °C in a humidified 5% CO_2 incubator. Confluent cells were washed with Hank's Balanced Salt Solution (HBSS) (Gibco), tripsinized, counted and then seeded at densities of (5×10^3 cells/ml). The 24 h assessment consisted in adding fresh media upon UVB exposure and incubating the cells for 24 h in a CO_2 incubator at 37°. This was followed by organelles damage assessment using the three cytotoxicity assays (NR, LDH and MTS).

Human Skin Fibroblasts were commercial cell cultures derived from human skin fibroblasts cells (GM05399). These cells were isolated from skin and maintained in cell culture. They were described as healthy non-fetal tissue derived from a 1-year-old male.

Non-tumorigenic Human Keratinocytes (HaCaT) were derived from normal keratinization in a spontaneously immortalized aneuploid human keratinocyte cell line [15].

2.2. Experimental design

Confluent cells in log phase of growth were released from the bottom of the culture flask using Trypsin EDTA, and then washed three times with cell culture medium. This was followed by a cell count before the cells were seeded on 24 well plates and incubated overnight to allow cells to reattach to the bottom of plates before UVB irradiation.

2.3. UVB exposure

The UVB irradiation procedure consisted in replacing culture medium with HBSS, the coverlids of the 24 well microtiter plate removed and cells exposed to UVB irradiation (3.92×10^{-4} W/cm^2) from a 6 lamps (FS40212) supplied by Wayne Electronics (Somerby, Australia) in a UV irradiation chamber (Fig. 1). The lamp output was measured by an IL-1700 research radiometer (International Light, Newburry Port, MA). Cells were irradiated with UVB doses ranging from 0 to 5.6 J/cm^2 [14].

2.4. In vitro cytotoxicity assays

2.4.1. MTS cell proliferation assay

UVB irradiated cells mitochondrial damage was assessed using the MTS assay (CellTiter 96® Aqueous non-radioactive cell proliferation kit, Promega). The method consisted in incubating the cell cultures with MTS-PMS [3-(4,5-dimethylthiazol-2-yl)-5-(3-carboxymethoxyphenyl)-2-(4-sulfophenyl)-2H-tetrazolium, inner salt-phenazine methosulfate] solution at 37 °C for 4 h in the dark. Upon incubation 100 μl of the supernatant was removed and transferred to a 96-well plate for reading at 492 nm using a Labsystem Multiskan MS plate reader (Finland).

2.5. Neutral red uptake assay

The NR assay was performed in 24-well plates (NUNC, Denmark) at 37 °C. The NR dye was filter-sterilized prior to use to prevent crystal formation. The assay was undertaken using the method described in Soni et al., 2010. Briefly NR was diluted 10 fold (0.33%) and added to the cell cultures for 2 h in a humidified CO_2 (4%) incubator (Sanyo, Japan) at 37 °C. Upon incubation cells were washed with HBSS and

treated with assay fixative (1% CaCl2:0.5% formaldehyde). The incorporated dye in the cells was dissolved in 300 ml of NRU assay solubilization solution (1% acetic acid: 50% ethanol) for 10 min. The colorimetric reaction was measured using the Labsystem, Multiskan MS reader at 540 nm. Background absorbance was measured (at 690 nm) and subtracted from the original reading to account for the corrected cell absorbance.

2.6. Lactate dehydrogenase assay

The assay measured the amount of lactate dehydrogenase released by the cells upon UVB insult (Promega Corporation). Released LDH in cultures was measured with a 30 min coupled enzymatic assay which resulted in the conversion of the tetrazolium salt into a red colored formazan product. The protocol supplied by Promega (Technical Bulletin 163) was followed without any alterations. 50 μl of the substances to be tested (HBSS in which the cells were exposed or the culture media where the cells were incubated for 24 h) was transferred to a 96 well plate. 12 ml of the assay buffer was mixed with the substrate mix and 50 μl of this solution added to each well of the plate. Cells were incubated for 30 min in the dark. This incubation period was followed by the addition of 50 μl of the stop solution (0.1 M HCl) to each well. The plates were spectrophotometrically read within 1 h at 492 nm.

2.7. Comet assay

The comet assay was performed using Trevigen comet assay silver staining kit. Briefly, Low melting agarose (LMA) container was uncapped and melted in a boiling water bath for 5 min before being placed at 37 °C water bath until ready for use. The prepared lysis solution was stored at 4 °C for 20 min before use. Cells at a density of 1×10^5 cells/ml were mixed with molten LMA (at 37 °C) at a ratio of 1:10 (v/v) and 75 ml immediately pipetted onto the comet slide, the side of the pipette tip was used to spread agarose and cells to ensure complete coverage of sample area. Slides were incubated at 4 °C in dark for 30 min for agarose solidification. Upon agarose solidification slides were immersed in the pre-chilled lysis solution at 4 °C for 60 min this was followed by slide tapped off to remove lysis solution before further immersion in freshly prepared alkaline solution for a period of 40 min at room temperature in dark. Slides were then gently taped and washed immersed in 1 X TBE buffer (pH 8.3) for 5 min prior to transfer to horizontal electrophoresis apparatus and aligned at equal distance from the electrodes. Slides immersed in Electrophoresis buffer (TBE, pH 8.3) were subjected to electrophoresis at 1 V cm^{-1} for 10 min. Upon electrophoresis completion, excess BE was tapped off and slide dipped in 70% ethanol for 5 min and air-dried to bring all cells in a single plan. Samples was desiccated overnight at room temperature for silver staining [6].

2.8. Comets silver staining

The silver staining method involved covering slide with 100 ml of fixation solution for 20 min at room temperature. The slide was then rinsed with deionized water for 30 min and sample area covered with 100 ml of staining solution for 5–20 min at room temperature until the comets acquired the desired intensity. The reaction was stopped by covering the samples with 100 ml of 5% acetic acid for 15 min followed by a deionized water wash. The slide was air-dried and stored in dark until ready for analysis.

2.9. Comets scoring and interpretation

The scoring of comet tail was based on DNA content (intensity) with untreated cells used as controls. DNA Silver staining generated a brown to black stain which could be observed under bright field microscopy. The DNA of untreated cells was confined to the nucleoid, as undamaged
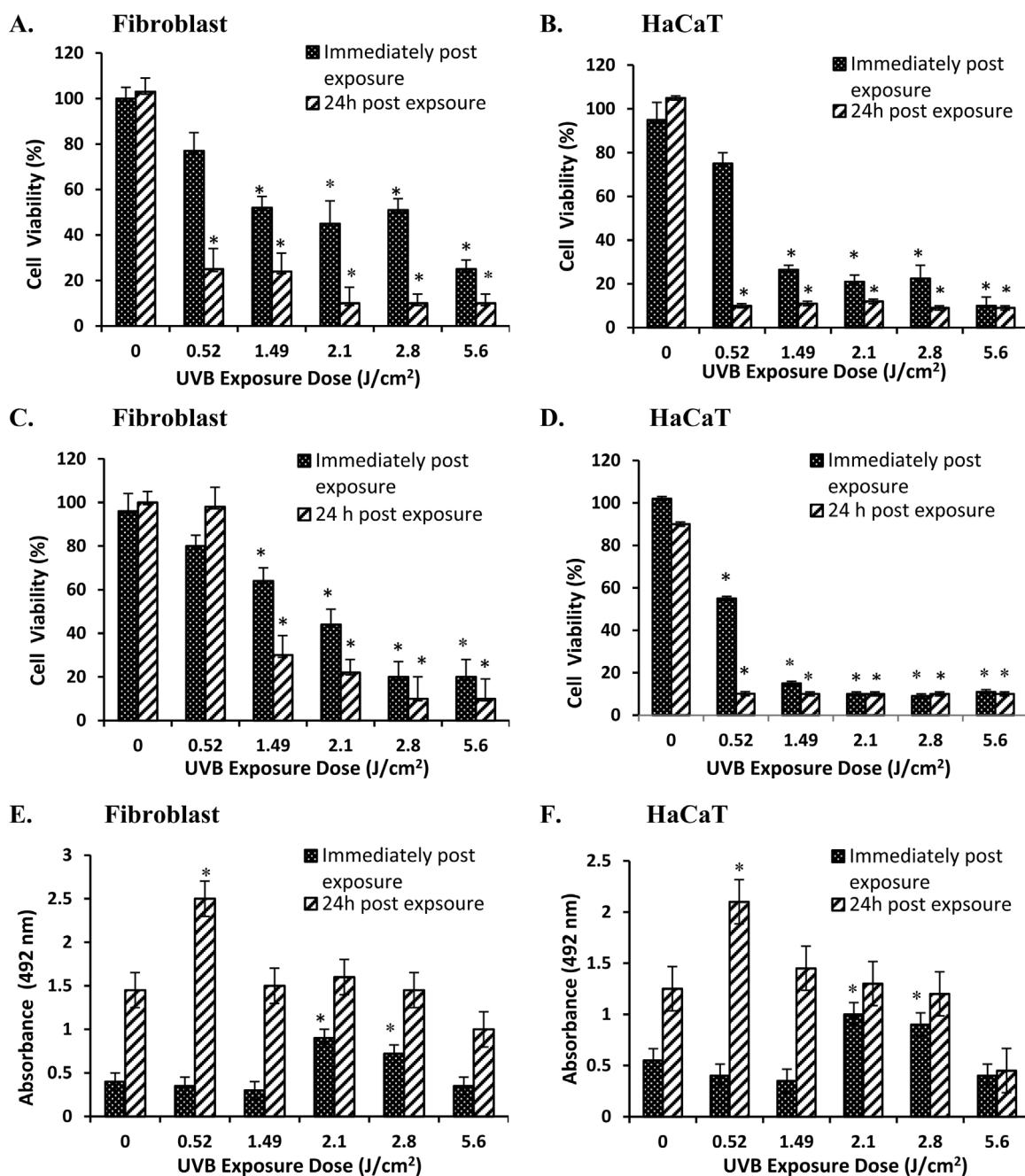
Fig. 1. Effects of UVB irradiation on cell viability. Fibroblasts and HaCaT cells were exposed to UVB doses ranging from 0 to 5.6 J/cm^2 immediately and 24 h post exposure as measured by the MTS assay (A and B), NR assay (C and D) and LDH assay (E and F). The effects of UVB irradiation on HaCaT LDH release immediately and 24 h post exposure as measured by the LDH assay. Data are expressed as% survival of cells. Data are the mean −SEM from three independent experiments. *P < 0.05 versus control group (non-irradiated).

DNA is supercoiled and does not migrate very far upon electrophoresis. In DNA-damaged cells (experimental and positive control) alkali treatment unwound the DNA which helped in its migration from nucleoid upon electrophoresis. The silver-stained comets resulting from exposure were analyzed using Comet Analysis Software Package (CASP). The CASP software generated many parameters such as head length, tail length, comet length, head DNA content, tail DNA content, tail movement and overall tail movement. The measuring parameters for the following − head center threshold, comet threshold, tail threshold and head threshold − were set at 0.95, 0.05, 0.1 and 0.05 respectively.

2.10. Western Blot

HaCaT cells were treated with two UVB doses (around the ED$_{50}$ values and double the ED$_{50}$ value). The adherent and non-adherent cells were collected on ice, washed twice with PBS, lysed with lysis buffer, and centrifuged at 12,000g for 10 min at 4 °C. The cell lysate was heated at 100 °C for 5 min, and the protein content was determined by the Bio-Rad protein assay (Bio-Rad, Hercules, CA, USA). Equal protein concentrations of each sample were loaded and resolved under reducing conditions by SDS-PAGE using 5% stacking gel, 10% separating gel and 1X running buffer (0.3% Tris Base, 1.4% glycine, 20% SDS, pH = 8.3) at 90 V for 30 min and then at 120 V for 2 h. Proteins were then transferred to PVDF membrane (Pall Corporation, Ann Arbor, USA) using semi-dry electro blotter (PEQLAB, Erlangen, Germany) and

1X transfer buffer (25 mM Tris base, 0.2 M glycine, 20% methanol, pH 8.5) at 10 V for 90 min. The membranes were blocked with blocking buffer (1X TBS, 0.1% Tween-20, 5% skim milk) for 2 h and then probed with primary rabbit polyclonal antibodies against actin, p53, p-p53, p21, Bcl-2, BAX, caspase-3, PARP, p38, p-p38, JNK, p-JNK, EGFR, p-EGFR, (Abcam, Cambridge, USA) at 4 °C overnight. Later, the primary antibodies were washed away with TBST for 1 h and the membranes were treated with horseradish peroxidase (HRP)-coupled secondary antibodies (Promega Corp., Madison, USA) for 1 h, and washed with TBST afterwards. Finally, Detection of each protein was performed using the ECL kit (Abcam plc, 330 Cambridge Science Park, Cambridge UK). Blot images were obtained with the image lab Software (BioRad, Chemidoc imaging instrument). The densitometer-intensity of single autoradiogram was determined using Quantity One software (Bio-Rad, Hercules, CA).

2.11. Statistical analysis

The *in vitro* data were expressed as the mean and S.D. for at least three different replicates (n = 3) at different exposures. Statistical procedures and graphical analysis were performed using Microsoft Excel software and SPSS software. Testing of the homogeneity of variances was conducted using the *f*-test and Student's *t*-test to compare exposed and control data. Differences were reported at statistically significant at $p < 0.05$.

3. Results

3.1. Establishing optimal cell number

Cells ranging in numbers from 10,000 to 80,000 cells/well were assessed using the MTS and NR assays. This was achieved by cell seeding different densities (10,000 to 80,000 cells/100 μl). The cells were allowed to re-attach to the bottom of the plate before conducting the experiments. Absorbance at 492 nm was performed at variable incubation times (0.5–3 h) to determine the optimal incubation time that could be picked for the MTS test without affecting the test accuracy. We selected the 2 h incubation with MTS as the optimal incubation time. The linearity of the colorimetric reaction was established by referring to the squared correlation coefficient (R^2). The R^2 was used to establish the Critical Cell Number Cutoff (CCNC) which represented the optimal number of cells to be used to keep the absorbance reading within the linear range. The CCNCs for fibroblasts and HaCaT cells for MTS and NR assays are summarized in Table 1 (R^2 values of 0.95 and above were used to select the CNCC).

3.2. Comparative cytotoxicity assessment using three in vitro assays

The CCNC data was used to determine the optimal cell seeding densities on 24 well plates prior to UVB irradiation. Cells were seeded on 24 well plates at the respective densities reported in Table 1 and allowed to attach for 24 h prior to irradiation. The sensitivity of the three assays in detecting UVB irradiation cellular (HaCaT and Fibroblasts) impact was investigated using the MTS, NR and LDH assays immediately and 24 h post exposure. The data is presented in Fig. 1.

HaCaTs and Fibroblasts were irradiated at different doses (0–5.6 J/cm²) and cell cytotoxicity at organelle level was assessed. The selection of HaCaT and Fibroblast cell lines was based on reported human skin penetration abilities of UVB. The studies reported radiation penetration as far as the dermis in UVB exposed human skin [16].

A dose dependent reaction was measured for UVB exposed cells using the NR, MTS and LDH extracellular release assays. It was evident from the MTS data that UVB exposure of skin fibroblasts and HaCaT cultures reduced the enzymatic mitochondrial dehydrogenase activity by up to 80% for doses of 5.6 J/cm² (immediately post exposure) as shown in Fig. 1A, B. This decrease in activity was more significant (doses as low as 0.52 J/cm²) when exposed cells were further incubated for 24 h (Fig. 1A, B).

The NR assay also detected significant changes induced by the UVB doses ranging from 0.52-5.6 J/cm² (Fig. 1C, D). The UVB exposure resulted in a dose dependent reduction in dye uptake by the exposed cells. This reduction agrees with the MTS data (Fig. 1A, B). The 24 h data results agreed with the MTS results whereby the two assays detected UVB cellular damages in both cell lines although the MTS assay was more sensitive in detecting damages for doses as low as 0.52 J/cm² in fibroblasts 24 h post exposure. The cellular damage measured at this dose with the NR assay did not show any significant decline at the 0.52 J/cm² dose. The inability of the neutral red assay to detect damage levels for doses of 0.52 J/cm² 24 h post exposure in fibroblast cells may be due to the nature of damage inflicted by irradiation which does not seem to affect cell membrane function as severely as it affects cellular mitochondrial metabolic functions. HaCaT cells irradiation data (Fig. 1, D) indicated damages for doses as low as 0.52 J/cm², with more pronounced lysosomal organelle damages (by comparison to mitochondrial dehydrogenase data) reported 24 h post exposure with NR assay (Fig. 1D).

The data presented in Fig. 1 indicated that UVB irradiation at a dose of 5.6 J/cm² triggered major damages in fibroblasts and HaCaT cells immediately and 24 h post exposure. The main differences observed were at low irradiation (0.52 J/cm²) where fibroblast lysosomes (Fig. 1C) did not display significant levels of damages by comparison to the mitochondrial dehydrogenase data (Fig. 1.A). The lysosomal damage was more pronounced for doses higher than 1.49 J/cm². The data indicated a dose dependent impact on cellular organelle damages mainly, cell membrane (LDH data) lysosomes (NR data) and mitochondrial lactate dehydrogenase activity (MTS data). The Exposure Dose (ED$_{50}$) that kills 50% of the cells in the two assays (MTS and NR) were calculated and presented in Table 2.

The presented data showed that cellular damages triggered by low dose UVB irradiation could be best measured 24 h post exposure using any of the cell types with the MTS and NR assays (Table 2). Comparing the ED$_{50}$ data for the two cell types 24 h post exposure revealed higher lysosomal damage levels (as measured by NR) at lower UV doses by comparison to mitochondrial lactate dehydrogenase damages.

Cell exposure to 2.1 J/cm² UVB dose triggered a significant increase in LDH release in both fibroblasts and HaCaT cells immediately post exposure. At doses higher than 2.1 J/cm² the measured LDH levels were decreasing. Further incubation of cells for 24 h led to significant LDH

Table 1
Critical cell number cutoffs for the MTS and NR assays for the different cell types used (Fibroblasts and HaCaT cells).

	Critical cell number cutoffs (cells/100 μl)	
	MTS assay	Neutral red assay
Fibroblasts	50,000	50,000
HaCaTs	80,000	80,000

Table 2
Calculated ED$_{50}$ for human cells using *in vitro* assays.

	UVB Dose Range J/cm²(0.70-5.63)	
	[ED$_{50}$][1](J/cm²) ± SD (J/cm²)	
Fibroblasts	Immediately	24 h post
MTS	1.72 ± 0.17	0.57 ± 0.03
NR	2.01 ± 0.14	0.38 ± 0.03
HaCaT		
MTS	0.79 ± 0.10	0.38 ± 0.20
NR	0.52 ± 0.10	0.28 ± 0.11

[ED$_{50}$] [1] value in this table represents the mean of three repetitive in J/cm².
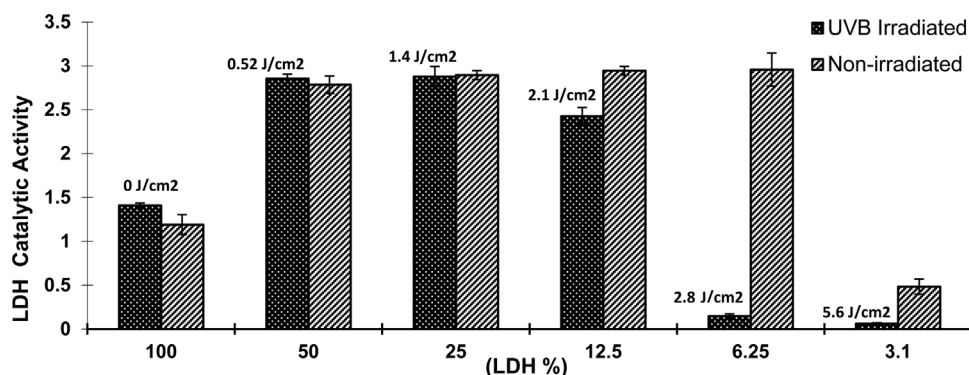
release peaking at a dose of 0.52 J/cm^2 in the two cell lines with a further loss of activity at higher doses. This observed reduction of LDH release at higher doses did not agree with damages reported with the MTS and NR assays in the two cell types. Further analysis of the data led us to hypothesize that this decrease in LDH levels could be the result of cellular activity being severely impaired from UVB exposure (Fig. 1A, B, C, D). Another plausible explanation to support low LDH levels detected for doses of UVB higher than 2.1 J/cm^2 could be that LDH enzyme exposure at low concentrations to UVB was leading to loss of catalytic activity. This assumption was tested through serially diluting (100%, 50%, 25% 12.5%, 6.25% and 3.10%) of an LDH positive control stock (0.066u/ml) and exposing it to various UVB doses (Fig. 2).

The data in Fig. 2 clearly indicates a substantial loss of LDH activity at very low dilution (6.25% and 3.10%) and at doses of 2.8 J/cm^2 and higher. This loss of activity explains the observed drop in LDH release at high UVB exposures. Thus the decrease in the LDH release was the result of cellular viability decline combined with LDH denaturation by UVB irradiation (Fig. 1E and F). This is in agreement with previous report demonstrating a similar decrease in the LDH activity post UV exposure [17].

3.3. Comet assay

Low doses of UVB plays a major role in the pathogenesis of skin cancer due to its capacity to induce immunosuppression and DNA damage in cells [18]. Therefore, there was a critical need to assess DNA damage onset and progression as a result of exposure using the comet assay. This protocol provided a simple and effective method for evaluating DNA damage in human cells. The experimental design aimed to check progression of DNA damage in HaCaT cells upon UVB insult. The choice of HaCaT cells stems from the important critical role keratinocytes play in protecting the skin from UVB irradiation. The quantitative and statistical data were generated using CASP software (Omar et al., 2007). Fig. 3A shows the typical silver-stained comets captured at various experimental conditions.

Tables 3 and 4 show qualitative and quantitative analysis of silver-stained comets on the basis of DNA damage of HaCaT cells immediately and 24 h post UVB exposure respectively.

The data in Tables 3 and 4 indicated a dose dependent DNA damage in UVB exposed cells with tail length, tail DNA contents and tail movement positively correlated to increased UV doses. In the negative control tail DNA content and length was minimal. Furthermore, UVB exposure higher than 4.32 J/cm^2 correlated nicely with our positive controls in the assay mainly KMnO$_4$ (Fig. 3A2). The conducted investigation suggested significant DNA damages from increased UVB dose conditions.

The results reported in Tables 3 and 4 are used to calculate the tail moment Index (TMI). The TMI consisted of selecting tail DNA content of cells at 4 and 24 h post exposure multiplied by the tail length and divided by 1000. The TM data is shown in Fig. 3B.

The TM analysis data indicated a dose dependent increase in the level of DNA damage as measured by the Comet assay. This agrees with the other cytotoxicity assays although we could detect significant DNA damages ($p < 0.05$) expressed at doses as low as 0.072 J/cm^2 24 h post exposure which could not be detected by any of the cytotoxicity battery of assays used. The absence of any damage recorded at very high doses 24 h post exposure is the result of the loss of all cells and inability to get cells for comet analysis. Therefore, our data suggested that early cellular damages appeared at the DNA level in the cells in the form of single breaks and followed by cell membrane damage and lastly organelle damages.

3.4. Western Blot

To explore the underlying apoptotic mechanisms resulting from UVB induced apoptosis, the expression levels of various pro-apoptotic and anti-apoptotic proteins in human keratinocytes (HaCaT) was evaluated by western blot analysis following UVB exposure below and above IC$_{50}$ for HaCaT cells. Cells were harvested at 4 h and 24 h post-UV irradiation and cell lysates were analyzed to detect the levels of Poly ADP ribose polymerase (PARP), pro-caspase-3, Bcl-2, Bcl-2-associated protein (BAX), p53, p-p53, p21 in relation to actin by western blotting. As shown in Fig. 4, a decrease in the level of pro-caspase-3 was obtained 4 h post UVB irradiation.

This decrease was more pronounced 24 h post UVB exposure. Similarly, UVB irradiation resulted in a significant PARP (116-kDa) cleavage to a PARP fragment (29-kDa). This was observed as a decrease in the expression level of PARP (116-kDa) concomitant with an increase in the level of cleaved PARP (29-kDa) specifically 24 h post UVB irradiation. The decrease in the level of procaspase-3 indicates that it was cleaved to an activated protease which in turn triggered proteolytic cleavage and inactivation of PARP leading to apoptotic cell death.

The results of the western blot analysis showed a dose-dependent decrease in the level of the anti-apoptotic protein Bcl-2 4 h following UVB exposure without a noticeable change in the levels of pro-apoptotic protein BAX. Moreover, HaCaT cells exposed to UVB (72 and 140 mJ/cm^2) showed significant decline in Bcl-2 levels and marked increase in BAX protein levels 24 h post treatment. These results also suggested that Bcl-2/BAX ratio would decrease after UVB irradiation which is an indication of mitochondrial or intrinsic apoptotic pathway. The relative expression of total and phosphorylated p53 protein was also assessed and the blots revealed a marked increase in p-p53 however a decrease in the total p-53 level was observed at 4 and 24 h post UVB irradiation as shown in Fig. 4. On the other hand, the expression level of the cell cycle inhibitor p21 protein which is under direct control of p53 was not altered 4 h post UVB irradiation. In contrast, the level of p21 decreased 24 h following UVB exposure. UVB-induced damage has been associated the phosphorylation of MAPK proteins. Maximum increases in the expression levels of both phosphorylated p38 and JNK were detected 4 h after UVB (72 and 140 mJ/cm^2) irradiation in HaCaT cells. On the contrary, this increase of JNK and p38 MAPK proteins was less significant 24 h following UVB exposure accompanied with a
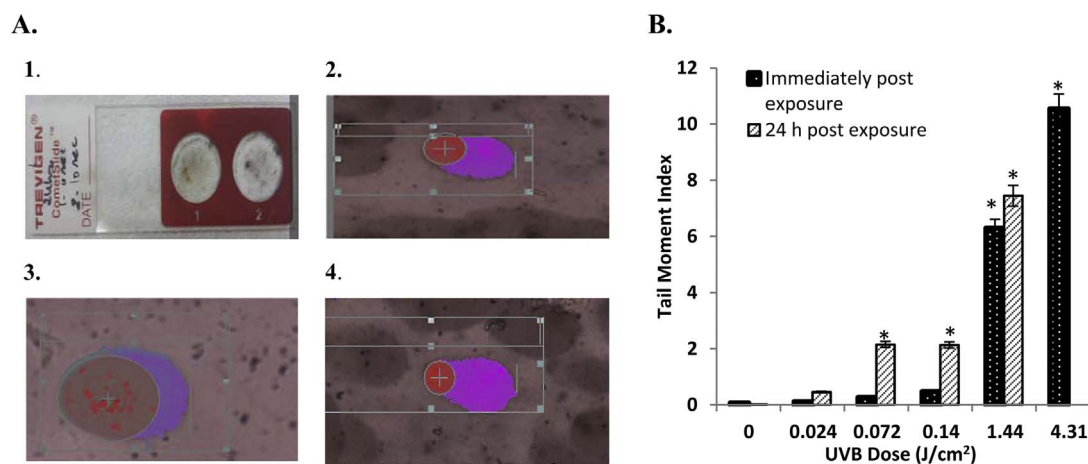
Fig. 3. DNA damage of HaCaT cells post UVB irradiation. (A.1) Typical comet slide captured after silver staining of UVB exposed cells. (A.2) Positive control consisted of DNA damaging agent (KMnO$_4$) at a concentration of 25 μM. (A.3) Negative control (non-irradiated cells). (A.4) Cells exposed to UVB irradiation. (B) Bar graphs showing the tail movement index of non-irradiated and irradiated cells. Data from Table 3 and 4 were chosen for tail moment analysis.

decrease in the total JNK and p38 proteins.

Previous studies have demonstrated that UV irradiation activates epidermal growth factor receptor (EGFR) and its downstream signaling target proteins such as MAPK pathway in skin keratinocytes (1, 2, 3). As shown in Fig. 5, UVB (72 and 140 mJ/cm^2) induced an increase in the level of phosphorylated EGFR (p-EGFR) 4 h and 24 h following UVB exposure, however, the level of total EGFR protein was slightly reduced 24 h after UVB irradiation. Based on these data, we conclude that EGFR plays a vital role in UV-induced JNK and p38 MAPK activation.

4. Discussion

UVB irradiation is considered the most important source of environmental damage to human skin [19]. A novel methodology for assessing UVB damage onset and progression in cultured human skin-derived cells (Fibroblasts and HaCaTs) was presented. The cytotoxicity and organelles damages resulting from UVB exposure was assessed with a battery of *in vitro* assays to establish damage levels in mitochondria, lysosomes, cell membrane, and DNA.

The cytotoxicity organelles damage assessment indicated dose dependent damages immediately post exposure with better assay sensitivity in picking up damages at lower irradiation 24 h post exposure (Fig. 1). This is in agreement with published literature [20,14] on damages reported 24 h post exposure) highlighting the damage triggered by exposure of cell cultures to UVB irradiation. The cytotoxicity data also indicated different sensitivities to UVB induced damage between the two cell types used. HaCaT cells appeared more sensitive as indicated by the MTS and NR assays.

The present results of acute UVB exposure indicated a dose dependent cellular damage expression as measured by the *in vitro* assays MTS, NR and LDH used. The organelles cellular damage agrees with previous published literature on the three assays [21–23]. The NR data also indicated a UVB dose dependent damage expression with a further presentation of damage 24 h post exposure. This agrees with previous

findings by other researchers [21] that reported a significant reduction of viability post UV exposure. The cytotoxicity assays selected in this study were successful in measuring damage levels but displayed different results immediately and 24 h post exposure. Immediately post exposure the more sensitive cell in detecting statistical significant damage levels ($p < 0.05$) were HaCaT cells using the NR assay. The 24 h post exposure data also indicated that HaCAT cells displayed the most statistical sensitivity ($p < 0.05$) with either of the assay system used.

The LDH data also indicated significant cell leakages upon UVB insult immediately and 24 h post exposure. We have reported a twofold significant increase in LDH release upon UVB insult at doses of 0.52 J/cm^2 24 h post exposure ($p < 0.05$) (Fig. 1). This was in agreement with previous study which revealed an 8 fold increase in LDH leakages for doses of 0.72 J/cm^2 post UVB exposure [21].

The comparative assessment of data generated by the three cytotoxicity assays used clearly indicated subtle differences in damage levels at organelles levels. These discrepancies in damage levels measurement were expected due to the nature of the assays used. LDH assay for example is measuring enzyme release into the supernatant post UVB insult rather than enzymatic mitochondrial activity (MTS) or uptake of dye by functional lysosomes (NR).

To summarize, the overall analysis of the *in vitro* cytotoxicity data clearly indicated that UVB appears to severely impact HaCaT cells that were the most sensitive to damage. In these cells it appears that lysosomal activity was severely impacted (Fig. 1D) immediately and 24 h post exposure at doses of 0.52 J/cm^2 and this was followed by mitochondrial activity and LDH release (Fig. 1B, D and F). The fibroblast cells appeared to be more resistant to organelles damages at 0.52J/cm^2 exposure with no statistical differences observed at this dose in the two cell lines with the exception of the 24 h post exposure data of Fibroblasts with MTS. The observed resistance to low UVB doses displayed by fibroblast could possibly be explained by the untransformed nature of the fibroblasts which makes them more robust at low UVB irradiation. Therefore, all the *in vitro* assays selected in this study successfully

Table 3
DNA damage in UVB exposed HaCaT as measured by the comet assay immediately (4 h) post exposure with CASP (Comet assay Software package).

UVB Dose (J/cm^2)	0	0.024	0.072	0.14	1.44	4.31
Head length	129 ± 8.01	210.33 ± 12.34	175.66 ± 29.03	198.33 ± 26.64	133.66 ± 3.71	107.66 ± 7.51
Tail length	22.33 ± 6.06	28 ± 2.51	38 ± 12.85	60 ± 10.69	112.33 ± 22.28	154.66 ± 15.07
Comet length	151.33 ± 9.90	238.33 ± 9.90	213.66 ± 31.79	258.33 ± 26.67	246 ± 18.90	262.33 ± 21.33
Head DNA content	97.08 ± 1.51	95.90 ± 0.81	93.04 ± 2.59	92.10 ± 0.76	54.36 ± 8.19	31.89 ± 2.16
Tail DNA content	2.91 ± 1.51	4.09 ± 0.81	6.95 ± 2.59	7.89 ± 0.76	45.63 ± 8.19	68.10 ± 2.16
Tail movement	0.80 ± 0.57	1.16 ± 0.28	3.29 ± 2.12	4.70 ± 0.91	54.91 ± 18.12	104.68 ± 6.66
Overall tail movement	1.82 ± 0.91	4.50 ± 1.13	6.11 ± 2.21	7.78 ± 0.37	42.13 ± 9.76	61.61 ± 3.98

Table 4

DNA damage analysis of UVB exposed HaCaT as measured by the comet assay 24 h post exposure with CASP (Comet assay Software package).

UVB Dose (J/cm^2)	0	0.024	0.072	0.14	1.44	4.31
Head length	97.66 ± 10.47	158.33 ± 18.55	85 ± 9.45	104.33 ± 18.70	159.66 ± 21.61	No cells found
Tail length	7.66 ± 4.17	42.335.364	62 ± 8.88	51.33 ± 5.89	146 ± 10.01	No cells found
Comet length	105.33 ± 14.33	200.66 ± 17.94	147 ± 15.94	155.66 ± 12.83	305.66 ± 31.46	No cells found
Head DNA content	97.51 ± 1.68	89.20 ± 5.19	65.27 ± 5.79	59.33 ± 8.36	49.41 ± 2.01	No cells found
Tail DNA content	2.48 ± 1.68	10.79 ± 5.19	34.72 ± 5.79	40.66 ± 8.36	50.58 ± 2.01	No cells found
Tail movement	0.32 ± 0.29	5.05 ± 2.94	21.98 ± 6.04	21.85 ± 7.15	73.45 ± 2.35	No cells found
Overall tail movement	1.25 ± 0.97	7.98 ± 3.89	16.37 ± 3.19	22.56 ± 1.30	62.39 ± 7.40	No cells found

measured UVB induced cellular damages and there is a need to use them in conjunction to try to differentiate between cell toxicity and organelles specific damages.

Our findings using the comet assay to measure DNA damage also indicated the suitability of the assay for measuring genotoxicity through assessment of DNA damages. The use of the comet assay in assessing DNA damages in HaCaT cells was confirmed by many researchers [24,25]. The comet assay results especially the TMI analysis (Fig. 4) clearly indicated that UVB exposure is triggering significant dose dependent DNA damages in HaCaT at doses as low as 0.072 J/cm^2 ($p < 0.05$). These results were in agreement with published literature on DNA damages caused by UVB irradiation in HaCaT cell cultures [26,27]. Previous studies indicated that exposure of skin cells to UV irradiation leads to cell death and apoptosis via the contribution of several independent signaling pathways mainly DNA damage, death receptor activation and ROS formation as well as the involvement of the mitochondria as coordinators of UV-induced apoptosis [28–30].

To gain an understanding of the mechanisms controlling UVB

induced apoptosis we examined several components of the apoptotic pathways. Caspase family of proteases participates in the regulation and execution of cell death by apoptotic stimuli [31]. Caspases are manufactured as zymogens (inactive precursors) in resting cells; however, following exposure to apoptotic stimuli, they become activated via partial proteolytic cleavage. Active caspases then cleave several downstream proteins, including PARP, leading to the execution of apoptosis [31]. This nuclear enzyme is involved in DNA repair and maintenance of genomic integrity and it has been used as an important marker of apoptosis [32]. Western blot results revealed that cleavage of caspase 3 has occurred as early as 4 h post-UVB irradiation. However, PARP remained uncleavaged (116-kD) 4 h after irradiation, but cleaved fragment (29-kD) became apparent 24 h post-UVB exposure, indicative of apoptosis induction. Earlier studies have shown that UVB radiation triggers the activation of both the intrinsic and extrinsic pathways [33–35]. Conversely, evidence suggests that the UVB-induced apoptosis of human keratinocytes is mainly mediated by the intrinsic pathway [36,37]. To evaluate the involvement of the mitochondrial (intrinsic)
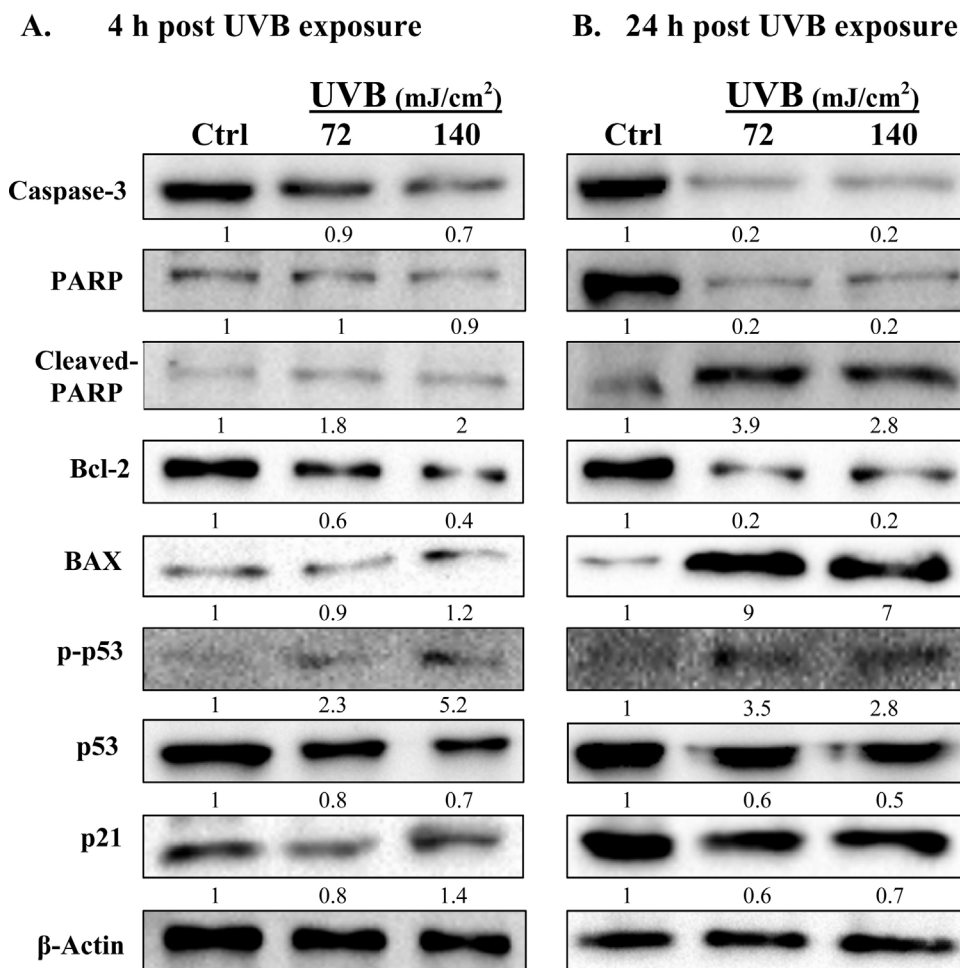
Fig. 4. Effects of UVB irradiation on the expression of apoptosis-related proteins in HaCaT cells. The HaCaT cells were irradiated at 72 and 140 mJ/cm^2 in HBSS and harvested at 4 h (A) and 24 h (B) post-UV irradiation. The expression levels of procaspase, PARP, Bcl2, BAX, p-p53, p53 and p21 were analyzed by western blotting. Expression of β-actin was used as an internal control. The densitometer-intensity of each band was determined relative to the bands of β-actin and is shown under the immunoblot as a fold change compared with non–UVB-exposed control, which has been assigned the arbitrary unit 1. Western blots are representative of three independent experiments.

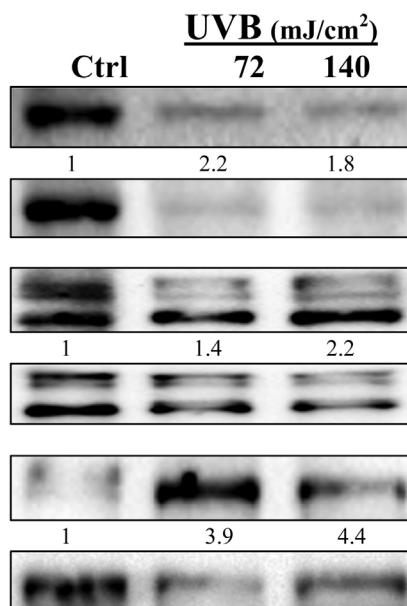**A. 4 h post UVB exposure**
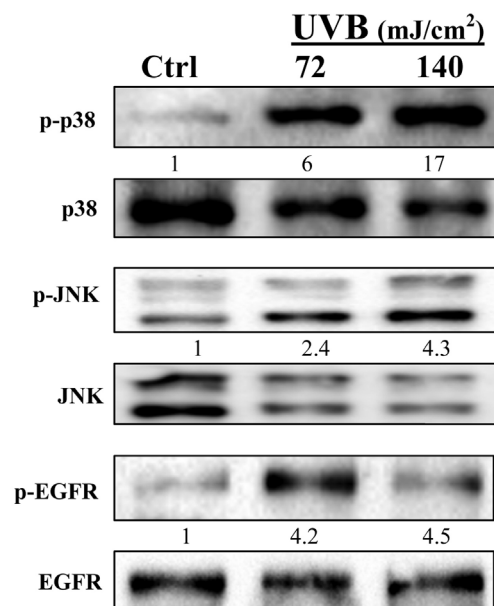
B. 24 h post UVB exposure

Fig. 5. Effect of UVB irradiation on the expression of MAP kinase and EGFR proteins in HaCaT cells. HaCaT cells were irradiated at 72 and 140 mJ/cm^2 in HBSS and harvested at 4 h (A) and 24 h (B) post-UV irradiation. The expression levels of total and phosphorylated p38, JNK kinases and EGFR were analyzed by western blotting. The densitometer-intensity of each band of phosphorylated proteins was determined relative to the bands of total proteins and is shown under the immunoblot as a fold change compared with non–UVB-exposed control, which has been assigned the arbitrary unit 1. Western blots are representative of three independent experiments.

pathway in the process of UVB-induced cell death, we analyzed the expression levels of Bcl-2 and BAX after UVB exposure. The proteins of the Bcl-2 family play an essential role in apoptosis and are considered as a target for anticancer therapy [38,39]. The Bcl-2 protein exhibits an anti-apoptotic effect while BAX is a pro-apoptotic protein of the Bcl-2 family [40,41]. Several studies have indicated that the ratio of Bcl-2 to BAX proteins decreases during apoptosis [42,43]. In this study, a decrease in the expression levels of Bcl-2 was obtained at 4 and 24 h post UVB irradiation, whereas, an increase in the expression level of BAX only appeared 24 h after UVB treatment. These results are in line with earlier studies which demonstrated that Bcl-2 overexpression prevents the UVB-induced apoptosis in human keratinocytes *in vitro* and *in vivo* [34,44]. It has been also reported that the decrease in the Bcl-2/BAX ratio favors apoptosis through release of the mitochondrial cytochrome c which sequentially activates caspase 3 [21].The tumor suppressor p53 plays an important role in response to DNA damage or other genomic instability and it is well established that activation of p53 can lead to cell cycle arrest or apoptosis [45]. Several studies indicated that elevated levels of p53 are detected post-UVB irradiation in various types of human skin cells [46,47]. In contrast, our western blot results of HaCaT cells harboring a mutant form of p53 showed a slight decrease in the expression level of p53 at 4 and 24 h following UVB exposure as well as a decrease in the level of p21 at 24 h post- UVB irradiation. The altered response in both proteins may be attributed to the presence of mutant p53 in these cells. However, despite the mutant form of p53, its activation to phosphorylated form after UVB irradiation was not affected. This suggests that pathways other than p53 must be involved in UV-induced apoptosis of keratinocytes or p53 protein may mediate UVB-induced apoptosis through pathways independent of transcription. The present findings are in accordance with previous reports indicating that p53 mediates mitochondria dependent apoptosis via direct interaction with the mitochondrion itself and/or with apoptotic related proteins of the Bcl-2 family. This involves the translocation of p53 to mitochondria followed by selective binding to and inhibition of the anti-apoptotic proteins Bcl-2 and Bcl-xL or activation of pro-apoptotic protein BAX [48,49].

UV irradiation has been shown to stimulate several members of the MAPK superfamily, comprising ERKs, JNKs, and p38 MAPK [50,51]. Numerous reports indicated that UVB causes a significant activation of both JNK and p38 MAPK in human keratinocytes [52,53]. It has been

shown that p38 MAPK pathway mediates apoptosis following UVB irradiation by inducing the release of mitochondrial cytochrome c into the cytosol, which is followed by pro-caspase-3 activation [33,52]. Furthermore, p38 MAPK activation by UVB is essential for the activation/translocation of BAX from the cytosol to mitochondria leading to cytochrome c release and intrinsic apoptotic pathway in UVB irradiated cultured keratinocytes as well as in human skin [13]. This was in line with our results which revealed that p38 and JNK activation was prominent 4 h post-UVB irradiation (Fig. 4) and subsequent BAX activation 24 h post-UVB exposure. Our results also demonstrated the activation of EGFR 4 h and 24 h post-UVB irradiation (Fig. 5). Previous studies indicated that EGFR is activated following UV irradiation and serves as an upstream signal in mediating UVB-induced downstream signal transduction including p38/JNK MAPK kinases [54,55].

In summary, the findings of this study demonstrated for the first time the utilization of *three in vitro* cytotoxicity methods as well as the comet assay to assess the damages on different cellular organelles immediately and 24 h post UVB irradiation. We concluded that damages expressed immediately post UVB exposures are magnified upon further incubation of irradiated cells for 24 h. Western blot analysis showed that UVB induced caspase dependent apoptotic cell death via the intrinsic mitochondrial pathway. Furthermore, UVB-induced apoptosis appears to be mediated through the activation of p38/JNK MAPK kinases.

Future research work will be focusing on elucidating the mechanisms triggered in human skin using Ex vivo skin and trying to correlate potential results to the *in vitro* results reported in this paper.

Conflict of interests

The authors declare that there is no conflict of interest regarding the publication of this paper.

Acknowledgments

References

[1] A. Svobodova, D. Walterova, J. Vostalova, Ultraviolet light induced alteration to the skin, Biomed. Pap. Palacky Univ. Olomouc 150 (1) (2006) 25.

[2] A. Kawano, A. Hayakawa, S. Kojima, M. Tsukimoto, H. Sakamoto, Purinergic signaling mediates oxidative stress in UVA-exposed THP-1 cells, Toxicol. Rep. 2 (2015) 391–400.

[3] J.A. Ruszkiewicz, A. Pinkas, B. Ferrer, T.V. Peres, A. Tsatsakis, M. Aschner, Neurotoxic effect of active ingredients in sunscreen products, a contemporary review, Toxicol. Rep. 4 (2017) 245–259.

[4] T.L. Fernandez, D.R. Van Lonkhuyzen, R.A. Dawson, M.G. Kimlin, Z. Upton, Characterization of a human skin equivalent model to study the effects of ultraviolet B radiation on keratinocytes, Tissue Eng. Part C: Methods 20 (7) (2014) 588–598.

[5] D. Kulms, T. Schwarz, Molecular mechanisms of UV-induced apoptosis, Photodermatol. Photoimmunol. Photomed. 16 (5) (2000) 195–201.

[6] B. Soni, N.P. Visavadiya, N. Dalwadi, D. Madamwar, C. Winder, C. Khalil, Purified c-phycoerythrin: safety studies in rats and protective role against permanganate-mediated fibroblast-DNA damage, J. Appl. Toxicol. 30 (6) (2010) 542–550.

[7] H.-Y. Jung, J.-C. Shin, S.-M. Park, N.-R. Kim, W. Kwak, B.-H. Choi, Pinus densiflora extract protects human skin fibroblasts against UVB-induced photoaging by inhibiting the expression of MMPs and increasing type I procollagen expression, Toxicol. Rep. 1 (2014) 658–666.

[8] Y.-K. Park, B.-C. Jang, UVB-induced anti-survival and pro-apoptotic effects on HaCaT human keratinocytes via caspase-and PKC-dependent downregulation of PKB: HIAP-1, Mcl-1, XIAP and ER stress, Int. J. Mol. Med. 33 (3) (2014) 695–702.

[9] G. Li, V. Ho, p53-Dependent DNA repair and apoptosis respond differently to high-and low-dose ultraviolet radiation, Br. J. Dermatol. 139 (1) (1998) 3–10.

[10] M. Leverkus, M. Yaar, B.A. Gilchrest, Fas/Fas ligand interaction contributes to UV-induced apoptosis in human keratinocytes, Exp. Cell Res. 232 (2) (1997) 255–262.

[11] L.L. Hill, A. Ouhtit, S.M. Loughlin, M.L. Kripke, H.N. Ananthaswamy, L.B. Owen-Schaub, Fas ligand: a sensor for DNA damage critical in skin cancer etiology, Science 285 (5429) (1999) 898–900.

[12] R. Takasawa, H. Nakamura, T. Mori, S. Tanuma, Differential apoptotic pathways in human keratinocyte HaCaT cells exposed to UVB and UVC, Apoptosis 10 (5) (2005) 1121–1130.

[13] A. Van Laethem, S. Van Kelst, S. Lippens, W. Declercq, P. Vandenabeele, S. Janssens, J.R. Vandenheede, M. Garmyn, P. Agostinis, Activation of p38 MAPK is required for Bax translocation to mitochondria: cytochrome c release and apoptosis induced by UVB irradiation in human keratinocytes, FASEB J. 18 (15) (2004) 1946–1948.

[14] C. Khalil, In vitro UVB induced cellular damage assessment using primary human skin derived fibroblasts, MOJ Toxicol. 1 (4) (2015) 20.

[15] P. Boukamp, R.T. Petrussevska, D. Breitkreutz, J. Hornung, A. Markham, N.E. Fusenig, Normal keratinization in a spontaneously immortalized aneuploid human keratinocyte cell line, J. Cell Biol. 106 (3) (1988) 761–771.

[16] W. Frain-Bell, Cutaneous Photobiology, Oxford University Press, USA, 1985.

[17] V. Artiukhova, M. Nakvasina, I. Lysenko, [Active forms of oxygen and the degree of UV modification of the structural and functional properties of lactate dehydrogenase] Radiatsionnaia biologiia radioecologiia/Rossiiskaia akademiia nauk 37 (3) (1996) 453–460.

[18] S. Lisby, R. Gniadecki, H.C. Wulf, UV-induced DNA damage in human keratinocytes: quantitation and correlation with long-term survival, Exp. Dermatol. 14 (5) (2005) 349–355.

[19] M. Brenner, V.J. Hearing, The protective role of melanin against UV damage in human skin, Photochem. Photobiol. 84 (3) (2008) 539–549.

[20] R. Calò, C.M. Visone, L. Marabini, Thymol and thymus vulgaris L. activity against UVA-and UVB-induced damage in NCTC 2544 cell line., mutation research/, Genetic Toxicol. Environ. Mutagen. 791 (2015) 30–37.

[21] S. Goyal, et al., Photosensitized 2-amino-3-hydroxypyridine-induced mitochondrial apoptosis via Smac/DIABLO in human skin cells, Toxicol. Appl. Pharmacol. 297 (2016) 12–21.

[22] C. Khalil, C. Winder, Surface water toxicity assessment by ecotoxicological and in vitro toxicologocial assays, WIT Trans. Ecol. Environ. 110 (2008) 253–262.

[23] S. Bakand, C. Winder, C. Khalil, A. Hayes, Toxicity assessment of industrial chemicals and airborne contaminants: transition from in vivo to in vitro test methods: a review, Inhal. Toxicol. 17 (13) (2005) 775–787.

[24] A.R. Collins, The comet assay for DNA damage and repair, Mol. Biotechnol. 26 (3) (2004) 249–261.

[25] S. Şardaş, N. Aygün, A. Karakaya, Genotoxicity studies on professional hair colorists exposed to oxidation hair dyes, Mutation Res. Genet. Toxicol. Environ. Mutagen. 394 (1) (1997) 153–161.

[26] K.C. Noz, M. Bauwens, P.P. van Buul, H. Vrolijk, A.A. Schothorst, S. Pavel, H.J. Tanke, B.J. Vermeer, Comet assay demonstrates a higher ultraviolet B sensitivity to DNA damage in dysplastic nevus cells than in common melanocytic nevus cells and foreskin melanocytes, J. Invest. Dermatol. 106 (6) (1996) 1198–1202.

[27] W.H. Poll, D. Hanelt, K. Hoyer, A.G. Buma, A.M. Breeman, Ultraviolet-B–induced cyclobutane-pyrimidine dimer formation and repair in arctic marine macrophytes, Photochem. Photobiol. 76 (5) (2002) 493–500.

[28] D. Kulms, T. Schwarz, Independent contribution of three different pathways to ultraviolet-B-induced apoptosis, Biochem. Pharmacol. 64 (5) (2002) 837–841.

[29] D. Kulms, E. Zeise, B. Poeppelmann, T. Schwarz, DNA damage: death receptor activation and reactive oxygen species contribute to ultraviolet radiation-induced apoptosis in an essential and independent way, Oncogene 21 (38) (2002) 5844–5851.

[30] Z. Assefa, A. Van Laethem, M. Garmyn, P. Agostinis, Ultraviolet radiation-induced apoptosis in keratinocytes: on the role of cytosolic factors, Biochim. Biophys. Acta (BBA)-Rev. Cancer 1755 (2) (2005) 90–106.

[31] I.N. Lavrik, A. Golks, P.H. Krammer, Caspases: pharmacological manipulation of cell death, J. Clin. Invest. 115 (10) (2005) 2665–2672.

[32] Z. Herceg, Z.-Q. Wang, Functions of poly (ADP-ribose) polymerase (PARP) in DNA repair: genomic integrity and cell death, Mutat. Res. Fundam. Mol. Mech. Mutagen. 477 (1) (2001) 97–110.

[33] Z. Assefa, A. Vantieghem, M. Garmyn, W. Declercq, P. Vandenabeele, J.R. Vandenheede, R. Bouillon, W. Merlevede, P. Agostinis, P38 mitogen-activated protein kinase regulates a novel, caspase-independent pathway for the mitochondrial cytochromec release in ultraviolet B radiation-induced apoptosis, J. Biol. Chem. 275 (28) (2000) 21416–21421.

[34] Z. Assefa, M. Garmyn, A. Vantieghem, W. Declercq, P. Vandenabeele, J.R. Vandenheede, P. Agostinis, Ultraviolet B radiation-induced apoptosis in human keratinocytes: cytosolic activation of procaspase-8 and the role of Bcl-2, FEBS Lett. 540 (1-3) (2003) 125–132.

[35] Y. Aragane, D. Kulms, D. Metze, G. Wilkes, B. Pöppelmann, T.A. Luger, T. Schwarz, Ultraviolet light induces apoptosis via direct activation of CD95 (Fas/APO-1) independently of its ligand CD95L, J. Cell Biol. 140 (1) (1998) 171–182.

[36] F. Chirico, C. Fumelli, A. Marconi, A. Tinari, E. Straface, W. Malorni, R. Pellicciari, C. Pincelli, Carboxyfullerenes localize within mitochondria and prevent the UVB-induced intrinsic apoptotic pathway, Exp. Dermatol. 16 (5) (2007) 429–436.

[37] A. Daher, C.M. Simbulan-Rosenthal, D.S. Rosenthal, Apoptosis induced by ultraviolet B in HPV-immortalized human keratinocytes requires caspase-9 and is death receptor independent, Exp. Dermatol. 15 (1) (2006) 23–34.

[38] J.B. Baell, D. Huang, Prospects for targeting the Bcl-2 family of proteins to develop novel cytotoxic drugs, Biochem. Pharmacol. 64 (5) (2002) 851–863.

[39] D.S. Goodsell, The molecular perspective: bcl-2 and apoptosis, Oncologist 7 (3) (2002) 259–260.

[40] T.W. Sedlak, Z.N. Oltvai, E. Yang, K. Wang, L.H. Boise, C.B. Thompson, S.J. Korsmeyer, Multiple Bcl-2 family members demonstrate selective dimerizations with Bax, Proc. Natl. Acad. Sci. 92 (17) (1995) 7834–7838.

[41] R.M. Kluck, E. Bossy-Wetzel, D.R. Green, D.D. Newmeyer, The release of cytochrome c from mitochondria: a primary site for Bcl-2 regulation of apoptosis, Science 275 (5303) (1997) 1132–1136.

[42] S. Elmore, Apoptosis: a review of programmed cell death, Toxicol. Pathol. 35 (4) (2007) 495–516.

[43] I. Marzo, J. Naval, Bcl-2 family members as molecular targets in cancer therapy, Biochem. Pharmacol. 76 (8) (2008) 939–946.

[44] H. Takahashi, M. Honma, A. Ishida-Yamamoto, K. Namikawa, A. Miwa, H. Okado, H. Kiyama, H. Iizuka, In vitro and in vivo transfer of bcl-2 gene into keratinocytes suppresses UVB-induced apoptosis, Photochem. Photobiol. 74 (4) (2001) 579–586.

[45] A. Mirza, et al., Global transcriptional program of p53 target genes during the process of apoptosis and cell cycle progression, Oncogene 22 (23) (2003) 3645–3654.

[46] K. Yoon, R.C. Smart, C/EBPα is a DNA damage-inducible p53-regulated mediator of the G1 checkpoint in keratinocytes, Mol. Cell. Biol. 24 (24) (2004) 10650–10660.

[47] D. Decraene, P. Agostinis, A. Pupe, P. De Haes, M. Garmyn, Acute response of human skin to solar radiation: regulation and function of the p53 protein, J. Photochem. Photobiol., B 63 (1) (2001) 78–83.

[48] N.D. Marchenko, A. Zaika, U.M. Moll, Death signal-induced localization of p53 protein to mitochondria a potential role in apoptotic signaling, J. Biol. Chem. 275 (21) (2000) 16202–16212.

[49] J.E. Chipuk, T. Kuwana, L. Bouchier-Hayes, N.M. Droin, D.D. Newmeyer, M. Schuler, D.R. Green, Direct activation of Bax by p53 mediates mitochondrial membrane permeabilization and apoptosis, Science 303 (5660) (2004) 1010–1014.

[50] L. Butterfield, B. Storey, L. Maas, L.E. Heasley, c-Jun NH2-terminal kinase regulation of the apoptotic response of small cell lung cancer cells to ultraviolet radiation, J. Biol. Chem. 272 (15) (1997) 10110–10116.

[51] D. Peus, R.A. Vasa, A. Beyerle, A. Meves, C. Krautmacher, M.R. Pittelkow, UVB activates ERK1/2 and p38 signaling pathways via reactive oxygen species in cultured keratinocytes, J. Invest. Dermatol. 112 (5) (1999) 751–756.

[52] H. Shimizu, Y. Banno, N. Sumi, T. Naganawa, Y. Kitajima, Y. Nozawa, Activation of p38 mitogen-activated protein kinase and caspases in UVB-induced apoptosis of human keratinocyte HaCaT cells, J. Invest. Dermatol. 112 (5) (1999) 769–774.

[53] A. Tada, E. Pereira, D. Beitner-Johnson, R. Kavanagh, Z.A. Abdel-Malek, Mitogen-and ultraviolet-B-induced signaling pathways in normal human melanocytes, J. Invest. Dermatol. 118 (2) (2002) 316–322.

[54] C. Cao, et al., EGFR activation confers protections against UV-induced apoptosis in cultured mouse skin dendritic cells, Cell. Signal. 20 (10) (2008) 1830–1838.

[55] T.B. El-Abaseri, S. Putta, L.A. Hansen, Ultraviolet irradiation induces keratinocyte proliferation and epidermal hyperplasia through the activation of the epidermal growth factor receptor, Carcinogenesis 27 (2) (2006) 225–231.